Myofibroblasts revert to an inactive phenotype during regression of liver fibrosis

Tatiana Kisseleva[a,1], Min Cong[a], YongHan Paik[a,b], David Scholten[a,c], Chunyan Jiang[a], Chris Benner[d], Keiko Iwaisako[a], Thomas Moore-Morris[e], Brian Scott[a], Hidekazu Tsukamoto[f], Sylvia M. Evans[e], Wolfgang Dillmann[a], Christopher K. Glass[d], and David A. Brenner[a]

[a]Department of Medicine, [d]Department of Cellular and Molecular Medicine, [e]School of Pharmacy, University of California, San Diego, CA 92093; [b]Department of Medicine, Samsung Medical Center, Sungkyunkwan University School of Medicine, Seoul 135-720, Korea; [c]Department of Medicine III, University Hospital Aachen, Aachen 52074, Germany; and [f]Southern California Research Center for Alcoholic Liver and Pancreatic Diseases and Cirrhosis, Keck School of Medicine of the University of Southern California, Los Angeles, CA 90033

Edited* by Michael Karin, University of California, San Diego School of Medicine, La Jolla, CA, and approved April 11, 2012 (received for review February 1, 2012)

Myofibroblasts produce the fibrous scar in hepatic fibrosis. In the carbon tetrachloride (CCl_4) model of liver fibrosis, quiescent hepatic stellate cells (HSC) are activated to become myofibroblasts. When the underlying etiological agent is removed, clinical and experimental fibrosis undergoes a remarkable regression with complete disappearance of these myofibroblasts. Although some myofibroblasts apoptose, it is unknown whether other myofibroblasts may revert to an inactive phenotype during regression of fibrosis. We elucidated the fate of HSCs/myofibroblasts during recovery from CCl_4- and alcohol-induced liver fibrosis using Cre-LoxP–based genetic labeling of myofibroblasts. Here we demonstrate that half of the myofibroblasts escape apoptosis during regression of liver fibrosis, down-regulate fibrogenic genes, and acquire a phenotype similar to, but distinct from, quiescent HSCs in their ability to more rapidly reactivate into myofibroblasts in response to fibrogenic stimuli and strongly contribute to liver fibrosis. Inactivation of HSCs was associated with up-regulation of the anti-apoptotic genes Hspa1a/b, which participate in the survival of HSCs in culture and in vivo.

Chronic liver injury of any etiology produces fibrosis as a result of deregulation of the normal healing process with massive accumulation of extracellular matrix (ECM), including type I collagen (ColI) (1). Myofibroblasts are $ColI^+$ α-smooth muscle actin $(\alpha\text{-SMA})^+$ cells that produce the ECM scar in fibrosis. One of the most important concepts in clinical and experimental liver fibrosis is reversibility. Removal of the etiological source of the chronic injury in patients (e.g., hepatitis B virus, hepatitis C virus, biliary obstruction, or alcohol) and in rodents [carbon tetrachloride (CCl_4) or bile-duct ligation] produces regression of liver fibrosis and is associated with decreased cytokine and ECM production, increased collagenase activity, and the disappearance of myofibroblasts (1, 2). During regression of fibrosis, some myofibroblasts undergo senescence (3) and apoptosis (2). However, the number of apoptotic myofibroblasts and the fate of the remaining myofibroblasts in the recovering liver is unknown.

Hepatic stellate cells (HSCs), the liver pericytes that store retinoids, are a major source of myofibroblasts in hepatotoxic liver fibrosis (4). Liver injury results in activation of quiescent HSCs (qHSCs), which proliferate and undergo phenotypical and morphological changes characteristic of myofibroblasts. Removal of the injurious agent results in the clearance of activated HSCs (aHSCs) by the cytotoxic action of natural killer cells (1) and is linked to up-regulation of ligands of natural killer cell receptors NKG2D, MICA, and ULBP2 in senescent aHSCs (3). Although never demonstrated in vivo, studies in culture suggest that aHSCs can revert to a more quiescent phenotype (5), characterized by expression of adipogenic genes and loss of fibrogenic gene expression (5).

Using genetic labeling of aHSCs/myofibroblasts, we demonstrate here that some aHSCs escape cell death and revert to an inactivated phenotype that is similar to, but distinct from, the original quiescent HSCs, including their ability to more rapidly reactivate into myofibroblasts. Because reversibility of fibrosis has been reported in lungs (6) and kidneys (7), these concepts and approaches may be applicable to study of fibrosis of other organs and provide new targets for anti-fibrotic therapy.

Results

Regression of Liver Fibrosis Is Accompanied by Loss of Myofibroblasts. Our study was designed to determine the fate of aHSCs/myofibroblasts ($\alpha\text{-SMA}^+ColI^+$ cells) during regression of hepatic fibrosis. For this purpose, reporter Col-GFP mice, expressing collagen-α1(I) promoter/enhancer-driven GFP, were subjected to CCl_4-induced liver injury for 2 mo. After cessation of the toxic agent, mice recuperated for 1 or 4 mo, and regression of liver fibrosis was evaluated by measuring collagen deposition and myofibroblast number (Fig. 1 *A* and *B*). CCl_4-treated mice developed severe fibrosis with activated myofibroblasts (Fig. 1 *A* and *B*), which decreased markedly after 1 and 4 mo of recovery. After 1 mo recovery, hydroxyproline levels and expression of the fibrogenic genes collagen-α1(I) and α-SMA were significantly decreased, compared with CCl_4-treated mice ($7.8 \pm 1.2\%$ Col-GFP and $8 \pm 1.5\%$ α-SMA; Fig. 1*B*), confirming that CCl_4-activated myofibroblasts disappear during recovery from liver fibrosis. Thus, because Col-GFP mice undergo regression of liver fibrosis after 1 mo of recovery, it is appropriate to study the fate of aHSCs/myofibroblasts for this time period.

Hepatic Stellate Cells Are the Major Source of CCl_4-Activated Myofibroblasts. The contribution of aHSCs to liver myofibroblasts in CCl_4-treated Col-GFP mice was determined using flow cytometry of the isolated nonparenchymal liver cell fraction, which contains aHSCs/myofibroblasts, inflammatory cells, and endothelial cells (8). Myofibroblasts were identified by Col-GFP expression, and HSCs were identified by vitamin A expression (1, 4, 8) (detected at 405 nm as an autofluorescent signal quenched by a violet laser) (Fig. 1*C*; *SI Appendix*, Fig. S1). GFP^+ cells ($92 \pm 3\%$) coexpressed vitamin A, demonstrating that aHSCs represent the major population of fibrogenic myofibroblasts in CCl_4-injured liver, as predicted by previous qualitative studies (9). Therefore, aHSCs can be genetically labeled on the basis of specific up-regulation of type I collagen expression (*SI Appendix*, Fig. S2) in CCl_4-induced liver fibrosis because other cellular sources do not make a significant contribution to the myofibroblast population.

Some aHSCs Apoptose During Regression of Liver Fibrosis. We hypothesize that the disappearance of aHSCs/myofibroblasts during

Author contributions: T.K. and D.A.B. designed research; T.K., M.C., Y.P., D.S., C.J., K.I., and T.M.-M. performed research; T.K., B.S., H.T., S.M.E., W.D., C.K.G., and D.A.B. contributed new reagents/analytic tools; T.K., C.B., C.K.G., and D.A.B. analyzed data; and T.K. and D.A.B. wrote the paper.

The authors declare no conflict of interest.

*This Direct Submission article had a prearranged editor.

Freely available online through the PNAS open access option.

See Commentary on page 9230.

[1]To whom correspondence should be addressed. E-mail: tkisseleva@ucsd.edu.

This article contains supporting information online at www.pnas.org/lookup/suppl/doi:10.1073/pnas.1201840109/-/DCSupplemental.

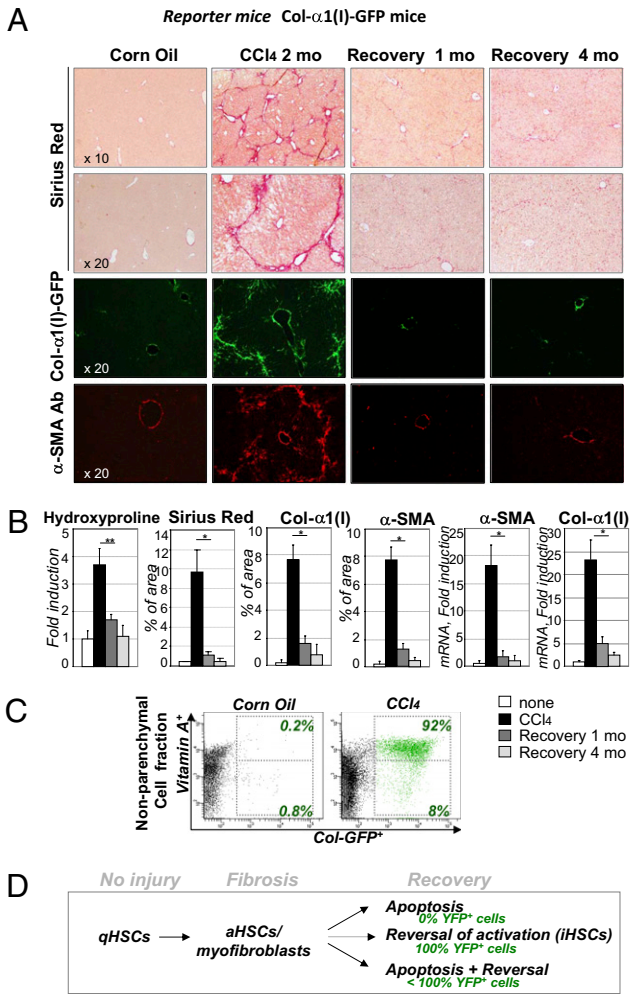

Fig. 1. Regression of liver fibrosis is accompanied by loss of myofibroblasts. (*A*) A comparison of the livers of Col-GFP mice that were untreated, CCl_4-treated (2 mo), or recovered from CCl_4 (1 and 4 mo) with respect to GFP expression, Sirius Red staining, and α-SMA immunohistochemistry. Representative bright-field and fluorescent micrographs are shown using 10× and 20× objectives. (*B*) Quantification of the same four groups in *A* with respect to hydroxyproline content, Sirius Red staining, α-SMA immunofluorescence, GFP expression, collagen-α1(I) mRNA level, and α-SMA mRNA level. $*P < 0.01$, $**P < 0.05$. (*C*) HSCs (vitamin A^+) constitute >90% of myofibroblasts (vitamin A^+GFP^+), as detected by flow cytometry of the nonparenchymal cell fraction from CCl_4-treated (2 mo) Col-GFP mice ($n = 3$). (*D*) Working hypothesis: CCl_4 induces activation of qHSCs into aHSCs/myofibroblasts. Cre-loxP–based genetic labeling marks the fate of collagen type I-expressing aHSCs/myofibroblasts (*SI Appendix*, Fig. S1). During recovery from CCl_4-liver fibrosis, aHSCs may (*i*) apoptose (no genetically labeled YFP^+ HSCs will remain in the liver) or (*ii*) inactivate (all YFP^+ cells survive) or (*iii*) some will apoptose and some will inactivate (YFP^+ iHSCs will number <100% of aHSCs).

regression of liver fibrosis may result from cell death by senescence (3) and apoptosis (2), inactivation, or both (Fig. 1*D*). Apoptosis of HSCs during regression of liver fibrosis is well documented (2). In agreement, we detected apoptotic aHSCs/myofibroblasts (2.6 ± 0.7%) by colocalization of cleavable caspase-3^+ and GFP^+ cells in the livers of Col-GFP mice 7 d after CCl_4 cessation, when apoptosis of hepatic cells was highest (*SI Appendix*, Fig. S3). Overall, early (7 d) recovery from liver fibrosis is accompanied by apoptosis of some aHSCs/myofibroblasts.

Genetically Labeled aHSCs/Myofibroblasts Persist in the Liver After 1 mo of Recovery from CCl_4. To determine if some liver myofibroblasts survive the regression of fibrosis, Col-α2(I)$^{Cre\text{-}YFP}$ mice [collagen-α2(I)^{Cre} × Rosa26$^{flox\text{-}Stop\text{-}flox\text{-}YFP}$ mice; *SI Appendix*, Fig. S2] were treated with CCl_4 (2 mo), allowed to recover (1 mo), and then analyzed for the persistence of genetically labeled YFP^+ cells (Fig. 2*A*). HSCs were identified by expression of GFAP and Desmin, and aHSCs/myofibroblasts were detected by expression of α-SMA. HSCs (98 ± 2%) were activated (e.g., upregulated YFP) in response to CCl_4 treatment, and YFP expression was detected in 94 ± 4% of myofibroblasts (α-SMA^+). Although myofibroblasts had completely disappeared in livers after 1 mo of recovery, YFP^+ cells surprisingly persisted. In particular, expression of YFP was detected in 38 ± 8% of Desmin$^+$ and 41 ± 5% of $GFAP^+$ cells, consistent with being HSCs that had been previously activated (Fig. 2*A*).

The immunohistochemistry (Fig. 2*A*) and flow cytometry (Fig. 2*B*) of gradient purified HSCs from Col-α2(I)^{YFP} mice identified three HSC phenotypes: (*i*) qHSCs (vitamin A^+ YFP^- α-SMA^-), (*ii*) aHSCs (vitamin A^+ YFP^+ α-SMA^+), and (*iii*) inactivated HSCs [(iHSCs), vitamin A^+ YFP^+ α-SMA^-]. After recovery from fibrosis, 56 ± 4% of HSCs coexpressed YFP^+ and vitamin A^+, indicating that these iHSCs had a history of type I expression but reverted to an inactivated phenotype (Fig. 2*B*).

Collagen-α2(I) and -α1(I) form a triple helix to produce collagen type I and are coexpressed in aHSCs/myofibroblasts (10). To provide independent confirmation of the above findings, we used Col-α1(1)$^{Cre\text{-}YFP}$ mice, generated by crossing collagen-α1(I)^{Cre} mice (*SI Appendix*, Fig. S4*A*) with Rosa26$^{flox\text{-}Stop\text{-}flox\text{-}YFP}$ mice. As expected, CCl_4 treatment of Col-α1(1)$^{Cre\text{-}YFP}$ mice produced aHSCs (Desmin$^+$$YFP^+$α-$SMA^+$ cells; *SI Appendix*, Fig. S4 *B* and *C*). Although α-SMA^+ myofibroblasts were no longer detected in livers after 1 mo recovery, 37 ± 9% of Desmin$^+$ HSCs still expressed YFP. In fact, genetically labeled YFP^+ HSCs persisted after 4 mo recovery (*SI Appendix*, Fig. S4*D*). Similarly, flow cytometry demonstrated that 38 ± 7% of YFP^+ vitamin A^+ HSCs expressed YFP after 1 mo recovery, compared with 83 ± 6% of YFP^+ vitamin A^+ aHSCs in fibrotic liver (*SI Appendix*, Fig. S4*E*). In the recovered liver, these iHSCs resided in the peri-sinusoidal space of Disse and exhibited a stellate shape (*SI Appendix*, Fig. S4*F*).

HSCs Transiently Express Collagen Type I During Development. Detection of YFP^+ qHSCs in Col-α2(1)$^{Cre\text{-}YFP}$ and Col-α1(1)$^{Cre\text{-}YFP}$ in adult livers before injury (Fig. 2*B*; *SI Appendix*, Figs. S4*E* and S5) may reflect transient collagen gene expression activating Cre during development. To prove this hypothesis, expression of collagen-α1(I) in real time was examined in livers of Col-GFP mice during embryogenesis (*SI Appendix*, Fig. S5). Indeed, transient expression of collagen-α1(I)-GFP was detectable in HSCs, identified by vitamin A, Desmin, and GFAP expression, between embryonic day 16.5 (E16.5) and postnatal day 14 (P14) (*SI Appendix*, Fig. S6*A*). At P14, 46 ± 8% of HSCs up-regulated collagen-α1(I)-GFP in real time but lacked α-SMA expression (*SI Appendix*, Fig. S6*B*). These GFP^+ HSCs did not exhibit characteristics of myofibroblasts (*SI Appendix*, Fig. S6 *C* and *D*), but were more similar to qHSCs than to aHSCs (*SI Appendix*, Fig. S6 *E* and *F*).

The fate of embryonic collagen$^+$ HSCs was examined in adult Col-α2(1)$^{Cre\text{-}YFP}$ mice (8 wk old). Consistent with our findings, YFP^+ qHSCs with a history of collagen expression and YFP^- qHSCs had identical gene expression profiles characteristic of a quiescent phenotype (*SI Appendix*, Fig. S6*E*).

Tamoxifen-Induced Genetic Labeling of aHSCs/Myofibroblasts in Adult Mice Confirmed Their Persistence in the Liver After 1 mo of Recovery from CCl_4. Tamoxifen-inducible Col-α2(1)$^{ER\text{-}Cre\text{-}GFP}$ mice were generated by crossing Col-α2(1)$^{ER\text{-}Cre}$ mice × Rosa26$^{flox\text{-}mTRed\text{-}Stop\text{-}flox\text{-}mGFP}$ mice (*SI Appendix*, Fig. S2). Genetic labeling of HSCs was achieved in adult CCl_4-treated Col-α2(1)$^{Er\text{-}Cre\text{-}GFP}$ mice by daily tamoxifen administration during the last week of CCl_4 treatment (*SI Appendix*, Fig. S7*A*). Genetically labeled aHSCs were visualized by loss of mTRed expression and gain of GFP expression upon Cre-loxP recombination. Desmin$^+$ HSCs (35 ± 6%) expressed GFP after CCl_4, and 14 ± 4% of HSCs were still GFP^+ after 1 mo recovery (Fig. 2*C*), confirming that CCl_4-activated HSCs (and their progeny) persist in the liver after regression of fibrosis. Consistently, GFP^+ iHSCs expressed Desmin, but not α-SMA (*SI Appendix*, Fig. S7*B*). Thus, three independent

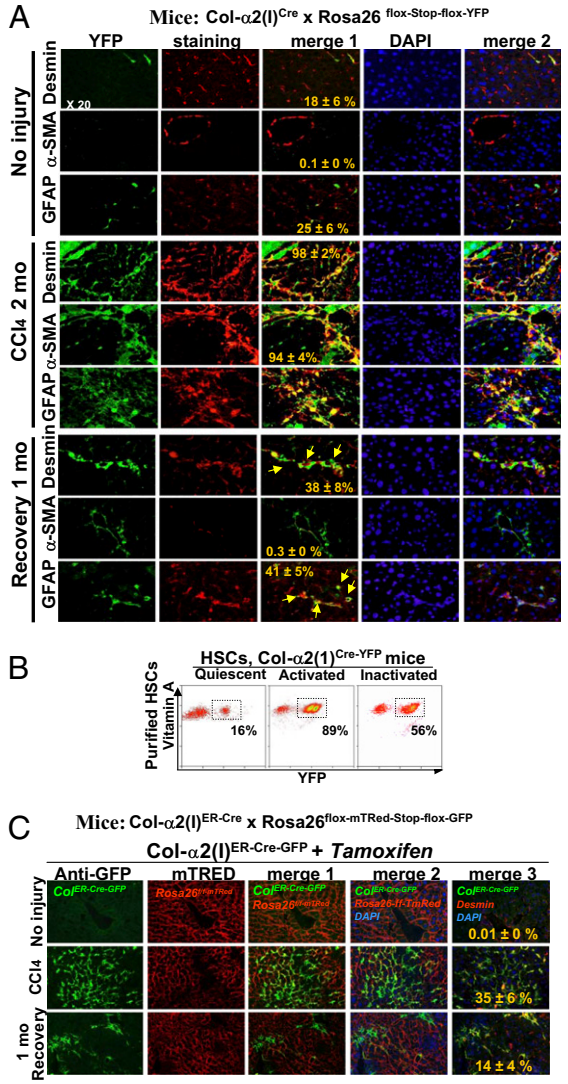

Fig. 2. Genetically labeled aHSCs persist after 1 mo recovery. (*A*) Livers from collagen-α2(I)$^{Cre\text{-}YFP}$ mice (no injury: n = 4; CCl_4-treated: n = 8; recovered: 1 mo n = 10) were costained for YFP, GFAP, Desmin, or α-SMA. Genetically labeled HSCs were identified after 1 mo recovery by YFP$^+$ expression in Desmin$^+$ or GFAP$^+$ cells. The number of YFP$^+$ HSCs is calculated relative to total HSCs (100%, merge 1, $P < 0.05$ comparing CCl_4 and recovery groups). Nuclei are shown (DAPI, merge 2). (*B*) HSCs (vitamin A$^+$) from collagen-α2(I)$^{Cre\text{-}YFP}$ mice (no injury: n = 4; CCl_4-treated: n = 6; recovered: 1 mo n = 6) were analyzed by flow cytometry. Genetically labeled aHSCs and iHSCs were identified by simultaneous vitamin A$^+$ and YFP$^+$ expression. Dot plots are shown; $P < 0.01$ (comparing YFP$^+$ aHSCs and YFP$^+$ iHSCs). (*C*) Genetically labeled GFP$^+$ HSCs persist in the livers of tamoxifen-inducible Col-α2(1)$^{ER\text{-}Cre\text{-}GFP}$ after 1 mo of recovery from CCl_4. To avoid genetic labeling of HSCs during development, tamoxifen-inducible Col-α2(1)$^{ER\text{-}Cre\text{-}GFP}$ mice were generated by crossing Col-α2(1)$^{ER\text{-}Cre}$ mice × Rosa26$^{flox\text{-}Stop\text{-}mTRed\text{-}flox\text{-}mGFP}$ mice (here labeled as Rosa26$^{f/f\text{-}mTRed}$ mice) and treated with CCl_4 (2 mo), and genetic pulse-labeling of aHSCs was induced by daily tamoxifen administration during the last week of CCl_4 treatment. After this treatment, mice recuperated for 1 mo to reverse liver fibrosis. Genetically labeled HSCs were visualized by immunostaining for membrane-tagged GFP$^+$ (and simultaneous loss of mTRed expression: merge 1), DAPI-stained nuclei (merge 2) were taken with a 20× objective. The number of genetically labeled GFP$^+$ HSCs was calculated as percentage of Desmin$^+$ HSCs (100%, merge 3). Genetic labeling of 35 ± 6% aHSCs was achieved in response to CCl_4. GFP$^+$ iHSCs (14 ± 4%) persisted in the liver after 1 mo recovery ($P < 0.05$; CCl_4 and recovery groups are compared), confirming that CCl_4-activated HSCs (and their progeny) remain in the liver after regression of fibrosis.

transgenic mice demonstrated that aHSCs/myofibroblasts revert to an inactive phenotype during regression of fibrosis.

Livers Recovering from Fibrosis Have Fewer HSCs. To quantify the number of HSCs during fibrosis and its regression, we generated GFAP$^{Cre\text{-}GFP}$ mice (GFAP^{Cre} mice × Rosa26$^{flox\text{-}Stop\text{-}mTRed\text{-}flox\text{-}mGFP}$ mice; *SI Appendix*, Fig. S8*A*). In uninjured mice, qHSCs were distributed throughout the hepatic acinus and represented 10.6 ± 0.8% of total liver cells. CCl_4 induced HSC activation, proliferation (14.3 ± 1.5% of total liver cells), and accumulation of aHSCs in the pericentral area. One month after recovery, the number of HSCs was reduced (5.6 ± 1.8% of total liver cells), and the distribution of HSCs was again similar to qHSCs. On the basis of immunostaining for GFAP after recovery from fibrosis in Col-α2(I)$^{Cre\text{-}YFP}$ and Col-α1(I)$^{Cre\text{-}YFP}$ mice (Fig. 2*B*; *SI Appendix*, Fig. S4*E*), iHSCs constitute 2% of total liver cells in the recovered liver (*SI Appendix*, Fig. S8*B*).

Genetically Labeled aHSCs/Myofibroblasts Persist in the Liver After 7 wk of Recovery from Alcohol-Induced Liver Fibrosis. We next determined if survival of aHSCs/myofibroblasts occurs during regression of alcohol-induced liver fibrosis. Liver fibrosis (and steatosis) was induced in Col-α2(I)$^{Cre\text{-}YFP}$ mice (collagen-α2(I)^{Cre} × Rosa26$^{flox\text{-}Stop\text{-}flox\text{-}YFP}$ mice) by intragastric alcohol feeding for 2 mo (*SI Appendix*, Fig. S9 *A* and *B*). Liver fibrosis (and steatosis) regressed in these mice 7 wk after withdrawal from ethanol feeding. Flow cytometry demonstrated that genetic labeling (YFP$^+$) was achieved in 64 ± 5% of myofibroblasts and persisted in 36 ± 4% of vitamin A$^+$ YFP$^+$ HSCs upon recovery from fibrosis (*SI Appendix*, Fig. S9*C*). Our findings were confirmed by immunohistochemistry (*SI Appendix*, Fig. S9 *D* and *E*). YFP expression persisted in 38 ± 7% of Desmin$^+$ HSCs/myofibroblasts following regression of liver fibrosis after withdrawal from ethanol despite the disappearance of myofibroblasts (α-SMA expressed in 1.4 ± 1% of YFP$^+$ HSCs/myofibroblasts; *SI Appendix*, Fig. S9*D*). Thus, two models of regression of liver fibrosis demonstrate survival of iHSCs.

iHSCs Demonstrate an Increased Response to Repeated Fibrogenic Stimuli. Purified iHSCs had a phenotype similar to that of qHSCs (Desmin$^+$, GFAP$^+$, Synemin$^+$, α-SMA$^-$; *SI Appendix*, Figs. S9*E* and S10). However, expression of myofibroblast-specific genes [Col-α1(I), α-SMA, TIMP-1] was induced more strongly in cultured TGF-β1–treated iHSCs than in qHSCs (Fig. 3*A*). In concordance, Col-GFP mice subjected to two rounds of CCl_4 injury separated by a 6-mo interval to allow complete recovery (2 × CCl_4) developed more severe fibrosis than littermates treated with one round of CCl_4 (1 × CCl_4; Fig. 3*B*). Thus, our in culture and in vivo data indicate that iHSCs with a history of activation are more effectively activated than qHSCs.

Adoptively Transferred HSCs (1-mo Recovery), but Not qHSCs, Contribute to Liver Fibrosis in Mice. To test this hypothesis, HSCs were isolated from Col-GFP$^+$/β-actin-RFP$^+$ mice that were uninjured and after 7 d and 1 mo recovery from CCl_4-induced fibrosis and adoptively transferred into livers of the newborn Rag2$^{-/-}$γc$^{-/-}$ mice (11) (Fig. 3*C*). One month later, these Rag2$^{-/-}$γc$^{-/-}$ mice were subjected to CCl_4 injury, and fibrotic livers were analyzed for the presence of GFP$^+$RFP$^+$ HSCs. Highest engraftment (70–78%) was achieved in mice transplanted with HSCs after 7 d or 1 mo recovery (versus 50% for qHSCs; *SI Appendix*, Fig. S11*A*). Unlike qHSCs, which were mostly scattered under the capsule or in liver parenchyma and constituted only 0.5 ± 0.2% of total HSCs, HSCs from the recovering livers were incorporated into the myofibroblast population in recipient mice and contributed 19 ± 2.3% and 13 ± 2.0% of total HSCs, respectively (Fig. 3*C*). Moreover, despite poor engraftment, comparable results were observed in CCl_4-treated wild-type mice adoptively transferred with qHSCs or HSCs (2 wk recovery) from Col-α1(I)$^{Cre\text{-}YFP}$ mice (*SI Appendix*, Fig. S11*B*). Taken together, iHSCs are primed to differentiate into myofibroblasts more rapidly in response to recurrent stimuli.

Inactivated HSCs Gradually Down-Regulate Collagen-α1(I). To further characterize iHSCs, Col-α1(1)$^{Cre\text{-}YFP}$ mice were crossed

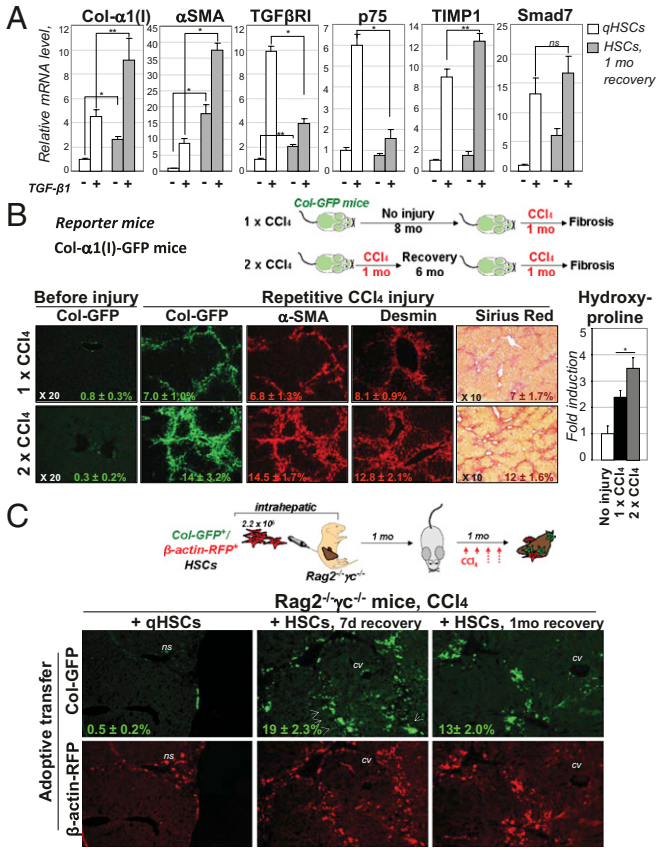

Fig. 3. HSCs (1 mo recovery) acquire a new phenotype distinct from qHSCs. (*A*) HSCs from Col-α1(1)$^{Cre\text{-}YFP}$ mice, uninjured or after 1 mo recovery, were cultured for 48 h ± TGF-β1 (2 ng/mL for 6 h), and analyzed by RT-PCR for expression of fibrogenic and neural genes; $*P < 0.01$, $**P < 0.05$. (*B*) CCl_4-treated Col-GFP mice (2 × CCl_4; $n = 4$) recuperated for 6 mo and were then subjected to recurrent CCl_4 injury. Development of liver fibrosis in these mice was compared with littermates treated with CCl_4 only the second time (1 × CCl_4; $n = 4$) by Sirius Red. The number of aHSCs was estimated by fluorescent microscopy for Desmin and α-SMA ($P < 0.05$, using 20× objective). Total collagen deposition was measured by hydroxyproline assay; $*P < 0.01$. (*C*) HSCs were isolated from collagen-α1(I)-GFP/β-actin-RFP mice, uninjured or after recovery (7 d or 1 mo) from CCl_4 injury, and transferred intrahepatically (2.2×10^5 cells) into 1-d-old Rag2$^{-/-}$γc$^{-/-}$ pups. Following CCl_4 injury, the number of RFP$^+$GFP$^+$ engrafted qHSCs and HSCs after 7 d and 1 mo was calculated relative to the number of total HSCs (detected by Desmin).

with Col-GFP mice, and genetically labeled HSCs (YFP$^+$) were analyzed for expression of collagen-α1(I) in real time (GFP$^+$; *SI Appendix*, Fig. S12). Following CCl_4 treatment (2 mo, *SI Appendix*, Fig. S12*A*), all YFP$^+$ HSCs expressed GFP. After 1 mo recovery from fibrosis, YFP$^+$ HSCs had decreased GFP expression. Similar results were obtained by flow cytometry (*SI Appendix*, Fig. S12 *B* and *C*), which allowed simultaneous detection of vitamin A, YFP, and GFP expression (12) in isolated HSCs. As expected, qHSCs lacked GFP expression and HSCs expressed GFP in response to CCl_4 (87 ± 5%; *SI Appendix*, Fig. S12*B*). Following a 2-wk recovery from CCl_4, decreased GFP expression was observed in 75 ± 3% of HSCs, of which 92 ± 4% still expressed YFP. The mean fluorescent intensity (mfi) of GFP expression was strongly reduced in YFP$^+$ HSCs at this time (~4 × 10^3 mfi, compared with aHSCs of ~6 × 10^4 mfi; *SI Appendix*, Fig. S12*B*). GFP expression (~1 × 10^3 mfi) decreased further in 42 ± 4% of HSCs after 1 mo recovery and correlated with the number of YFP$^+$ iHSCs (55 ± 3%). Thus, inactivation of HSCs occurs gradually and steadily during recovery from CCl_4-induced fibrosis. Interestingly, 45% of HSCs after 1 mo recovery had no history of collagen expression (YFP$^-$) and represent new qHSCs (*SI Appendix*, Fig. S12*B*).

iHSCs Acquire a New Phenotype Distinct from qHSCs. To assess changes in global gene expression, inactivated YFP$^+$ HSCs (iHSCs, 1 mo recovery) were evaluated by the whole-mouse genome microarray and compared with qHSCs, aHSCs, and HSCs after 7 d recovery (Fig. 4*A*). We confirmed that YFP$^+$ iHSCs down-regulated fibrogenic genes (Col-1α1, Col-1α2, Col-1α1, α-SMA, TGFβRI, and TIMP1) during recovery from fibrosis, but failed to obtain a quiescent phenotype [up-regulated peroxisome proliferator-activated receptor γ (PPARγ) and Bambi, but not the other quiescence-associated genes adipose differentiation relate protein (Adfp), Adipor1, or GFAP] (5) (Fig. 4*B*). Unsupervised clustering of gene expression profiles revealed that YFP$^+$ iHSCs (1

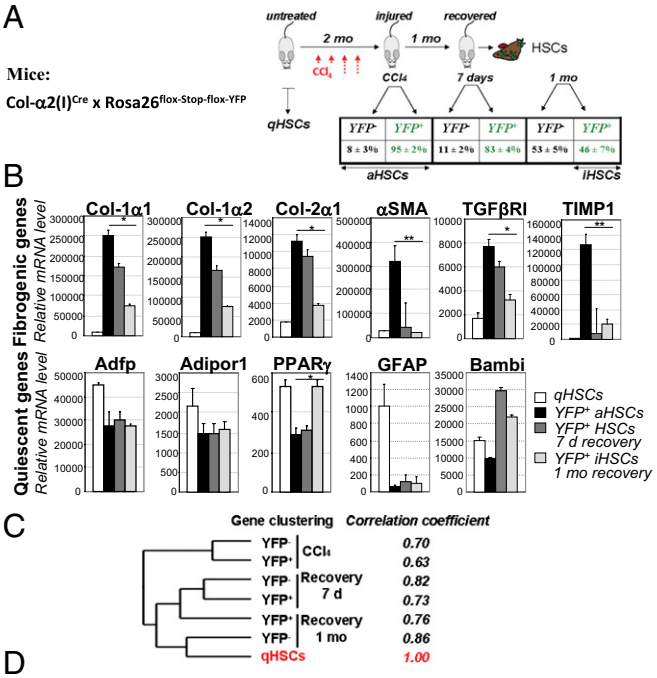

SIGNATURE GENES :			
Maximum ↑ YFP$^+$ iHSCs 1 mo	Fold	Maximum ↑ YFP$^+$ HSCs 7 d	Fold *
Cathepsin S	85	Keratin 20	14
CD74	66	Hspa1a	10
MHC class II (H2-Ab1)	42	Hspa1b	12
CXCL1	3.5	Glypican 3 (Gpc3)	5.5
CD52	31	Calpain 6	4
CCL4	31	midkine	3
CD83	29	MMP2	3
Integrin α X (Itgax)	18	Cyclin G2 (Ccng2)	3.6
Lectin (Lgals3)	12	PPARγc1a	2.7
CXCL10	11	Hspb2	2

Fig. 4. Genetically labeled HSCs obtain a new "inactivated" phenotype after 1 mo of recovery. (*A*) Microarray analysis. Vitamin A$^+$ HSCs were sort-purified from Col-α2(I)$^{Cre\text{-}YFP}$ mice that were untreated ($n = 6$), fibrotic ($n = 6$), after 7 d of recovery ($n = 3$), and after 1 mo of recovery ($n = 6$). YFP$^+$ and YFP$^-$ HSCs were then subjected to the Whole Mouse Genome Microarray. Representative cell number is shown for each HSC group. (*B*) YFP$^+$ iHSCs (1 mo recovery) down-regulate mRNAs of fibrogenic genes and up-regulate PPARγ and Bambi but not other qHSC genes (Adfp, Adipor1, GFAP). The results show the relative mRNA level (average of normalized values/multiple probes/gene) obtained using the Agilant microarray; $*P < 0.01$, $**P < 0.001$. (*C*) Gene expression profile clustering analysis identifies similarity between the different HSC phenotypes. The correlation coefficient was used to compare the qHSC (1.00) gene expression pattern with YFP$^+$ iHSCs (0.76) and aHSCs (0.63) expression patterns. (*D*) Expression of signature genes was determined for YFP$^+$ iHSCs (1 mo) and YFP$^+$ HSCs (7 d recovery, 7 d), and fold induction (compared with YFP$^+$ aHSCs) is shown for each group.

mo) exhibit an intermediate profile between that of qHSCs and YFP$^+$ HSCs (7 d recovery), but share more similarity to qHSCs than to aHSCs (Fig. 4 *C* and *D*). Similar results were obtained using correlation coefficient analysis comparing expression profiles to qHSCs (Fig. 4*C*) and unsupervised clustering of gene-specific expression profiles (*SI Appendix*, Fig. S13 *A* and *C*).

Activation of Heat-Shock Proteins 1a/b May Promote Survival of iHSCs at Day 7 of Recovery from Liver Fibrosis. To understand how YFP$^+$ iHSCs escape apoptosis, we examined the signaling pathways in YFP$^+$ HSCs after 7 d recovery (*SI Appendix*, Fig. S13 *B* and *E*). In particular, expression of the anti-apoptotic heat-shock proteins 1a/b (Hspa1a/b) genes was strongly but transiently induced in these HSCs (Fig. 5*A*; *SI Appendix*, Fig. S14*A*) to the levels comparable to qHSCs, but was dramatically down-regulated in aHSCs and HSCs after 1 mo recovery (Fig. 5*A*; *SI Appendix*, Fig. S14*A*).

We examined if Hspa1a/b would impact survival of cultured HSCs. For this purpose, HSCs were isolated from CCl_4-treated Hspa1a/b$^{-/-}$ and wild-type mice (*SI Appendix*, Fig. S14*B*) and cultured 5 d on plastic. Hspa1a/b$^{-/-}$ HSCs had a rounded shape and exhibited growth retardation (cell-number ratio knock out: wt: 1:1.7; *SI Appendix*, Fig. S14*C*). Moreover, Hspa1a/b$^{-/-}$ HSCs were more susceptible to glyotoxin- (13) and TNF-α–induced apoptosis (14) (Fig. 5*B*; *SI Appendix*, Fig. S14*C*). Therefore, up-regulation of Hspa1a/b genes may promote survival of iHSCs during recovery from fibrosis.

Resolution of CCl_4-Induced Fibrosis Is Expedited in Hspa1a/b$^{-/-}$ Mice. We hypothesized that the loss of survival signals in Hspa1a/b$^{-/-}$ HSCs would result in increased clearance of aHSCs after recovery from CCl_4-induced fibrosis. To test this, Hspa1a/b$^{-/-}$ and wild-type mice were subjected to CCl_4-induced liver injury. As expected, Hspa1a/b$^{-/-}$ mice developed more severe fibrosis (probably due to increased hepatocyte death) (15) than did the wild-type littermates (Fig. 5*C*). However, after stopping CCl_4 treatment, regression of liver fibrosis was strongly accelerated in Hspa1a/b$^{-/-}$ mice compared with wild-type mice (decreased 49 vs. 20%, respectively, by Sirius red staining). Hspa1a/b$^{-/-}$ livers also had a greater loss of α-SMA$^+$Desmin$^+$ aHSCs compared with wild-type mice (decreased 68 vs. 40% of Desmin$^+$ positive area, respectively; Fig. 5*C*). Thus, Hspa1a/b is required so that iHSCs persist in the recovering liver.

Discussion

Clinical and experimental hepatic fibrosis regresses dramatically with removal of the underlying etiological agent. Myofibroblasts are aSMA$^+$ collagen type I$^+$ cells that are absent from the normal uninjured liver, rapidly emerge in fibrotic liver to produce the fibrous scar, and completely disappear with regression of liver fibrosis (1, 2). In hepatotoxic-induced liver fibrosis (such as CCl_4 or intragastric alcohol feeding), quiescent hepatic stellate cells (GFAP$^+$Desmin$^+$SMA$^-$Col$^-$ qHSCs) undergo activation to become the major source of myofibroblasts (GFAP$^+$Desmin$^+$aSMA$^+$Col$^+$ aHSCs). Our study uses genetic markers to address the fate of these aHSCs/myofibroblasts during regression of liver fibrosis. We demonstrate that aHSCs/myofibroblasts are cleared by two mechanisms: (*i*) as previously reported, some myofibroblasts undergo cell death by apoptosis (2); and (*ii*) some myofibroblasts revert to a previously unrecognized inactive phenotype (iHSCs) that is similar to, but distinct from, quiescent HSCs.

Reversal of fibrosis is associated with increased collagenase activity, activation of macrophages/Kupffer cells secreting matrix metalloproteinases, and matrix degradation (1). Senescence and apoptosis of activated HSCs plays a significant role in resolution of liver fibrosis by eliminating the cell type responsible for producing the fibrotic scar (2, 3). Here we demonstrate that some aHSCs undergo apoptosis, whereas other aHSCs escape apoptosis, lose expression of fibrogenic genes, and persist in the liver in an inactivated phenotype. This phenomenon was demonstrated using two models of liver fibrosis with different etiologies: CCl_4- and alcohol-induced liver injury. These data suggest that inactivation of aHSCs/myofibroblasts is a common feature of regression of liver fibrosis.

Studies in culture suggest that aHSCs can revert to a quiescent phenotype, associated with expression of lipogenic genes (Adfp, Adipor1, CREBP, PPAR-γ) (5) and storage of vitamin A in lipid droplets. Depletion of PPAR-γ constitutes a key molecular event for HSC activation, and ectopic overexpression of this nuclear receptor results in the phenotypic reversal of activated HSC to quiescent cells in culture (5). The treatment of activated HSCs with an adipocyte differentiation mixture, overexpression of SREBP-1c, or culturing on basement membrane-like ECM (16) results in up-regulation of adipogenic transcription factors and causes morphologic and biochemical reversal of activated HSCs to quiescent cells (17). Our in vivo cell-fate mapping studies demonstrate that iHSCs survive apoptosis during reversal of liver fibrosis with a new phenotype that is similar to, but distinct from, the original qHSCs.

Our study confirms that HSCs transiently express collagen type I during development (E16.5–P14), but do not spontaneously become myofibroblasts. This observation explains the presence of genetically labeled qHSCs with a history of collagen expression in livers of uninjured adult mice. These genetically labeled qHSCs possess a quiescent phenotype, indistinguishable from qHSCs with no history of collagen expression. In addition, transient activation of HSCs is required for liver regeneration following partial

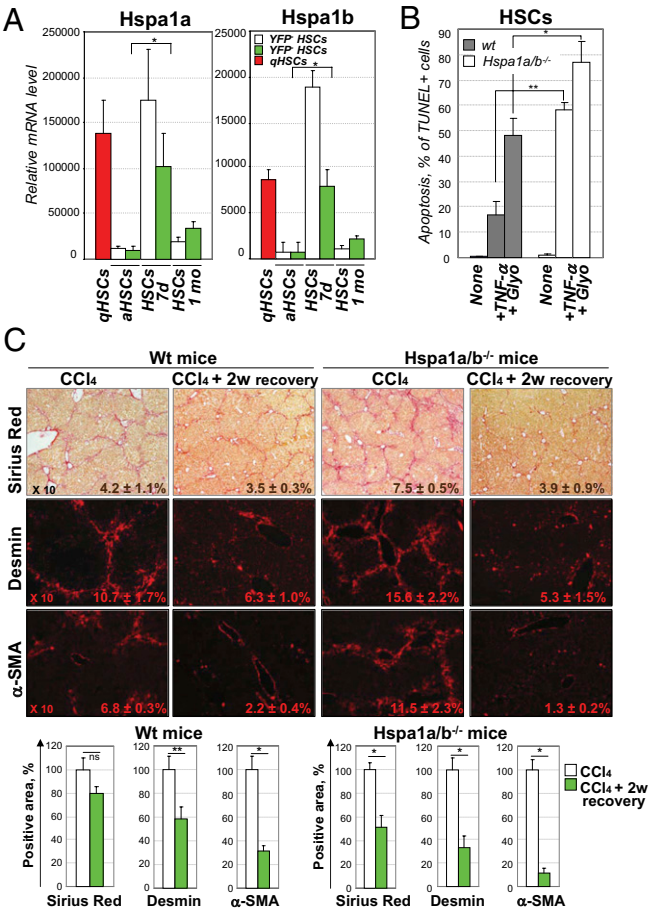

Fig. 5. Genetically labeled YFP$^+$ HSCs up-regulate prosurvival Hsp1a/b genes at 7 d of recovery. (*A*) Up-regulation of prosurvival Hsp1a/b genes in YFP$^+$ HSCs at 7 d of recovery. The results are expressed as relative mRNA levels (average of normalized values/multiple probes/gene; *$P < 0.001$) obtained by Agilant microarray. (*B*) Apoptosis was induced in Hspa1a/b$^{-/-}$ and wild-type HSCs by glyotoxin (25 nM for 4 h) and TNF-α (20 ng/mL) + actinomycin (0.2 μg/mL) for 18 h. (*C*) Hspa1a/b$^{-/-}$ and wild-type (Wt) mice were gradually subjected to CCl_4 injury and recovered for 2 wk, and livers were analyzed by Sirius Red, staining for Desmin and α-SMA (positive areas are indicated). Regression of fibrosis and disappearance of fibrogenic myofibroblasts during recovery were calculated in comparison with CCl_4 treatment (100%) and are shown as percentage of Sirius Red-, Desmin-, and α-SMA–positive areas; *$P < 0.01$, **$P < 0.05$.

hepatectomy (18), but the subsequent fate of these HSCs is currently unknown. In turn, after 1 mo of regression from CCl_4-induced liver fibrosis, aHSCs/myofibroblasts do not fully revert to a quiescent phenotype. iHSCs down-regulate the fibrogenic genes collagen-α1(I), collagen-α1 (2), α-SMA, TGFβRI, and TIMP1 and up-regulate some quiescence-associated genes (PPARγ and Bambi) to levels comparable to qHSCs, but do not reacquire high expression of GFAP, Adfp, and Adipor1 (5). These genetically labeled iHSCs constituted ∼50% of total HSCs in the liver 1 mo after reversal of liver fibrosis. Interestingly, the remaining HSCs have no history of activation, highly resemble qHSCs phenotypically, and represent new qHSCs generated from residual YFP^- qHSCs or from a precursor cell population. Although during development HSCs originate from submesothelial mesenchymal cells (19), the source of HSC replenishment is unknown. Using bone marrow chimeric mice, several studies have indicated that HSCs originate from endogenous liver cells and not from a bone marrow-derived progenitor cell (8).

Unlike aHSCs, iHSCs completely down-regulate expression of fibrogenic genes, but, in response to TGFβ1, more rapidly activate into myofibroblasts than qHSCs. Consistent with the concept of iHSCs being more fibrogenic than qHSCs, a previously injured and recovered liver develops more fibrosis than a naive liver. We then more directly tested this concept in vivo by adoptive transfer of HSCs into livers of immunodeficient $Rag2^{-/-}\gamma c^{-/-}$ mice. Unlike previous ectopic transfer experiments (20, 21), HSCs (1 mo recovery) were transplanted into their natural liver environment, and their response to CCl_4 injury was monitored. Here we demonstrate that iHSCs activate and fully integrate into the fibrous scar in recipient mice more efficiently than qHSCs. Thus, in culture and in vivo iHSCs are activated more effectively than naive qHSCs, so that the previously injured liver generates more fibrous scar in response to a repeated injury.

It is not clear why some aHSCs escape apoptosis and inactivate, whereas other HSCs die after cessation of the injury. Our study suggests that survival of iHSCs requires the up-regulation of prosurvival signals, such as induction of heat-shock proteins (22). Two members of the Hsp70 family of heat-shock proteins, Hspa1a and Hspa1b (22), which play a protective role against stress-induced apoptosis (23), were strongly and transiently up-regulated in HSCs after 7 d of reversal of fibrosis (when apoptosis of other aHSCs is highest) compared with the aHSCs in fibrotic liver. Furthermore, we demonstrate that genetic ablation of Hspa1a/b renders aHSCs more susceptible to TNF-α (14) and glyotoxin-induced (13) apoptosis in culture. In concordance, regression of liver fibrosis was strongly accelerated in $Hspa1a/b^{-/-}$ mice and was associated with increased disappearance of α-$SMA^+Desmin^+$ HSCs. We can speculate that Hspa1a/b regulate HSC survival, whereas PPAR-γ drives HSC inactivation during reversal from liver fibrosis.

Materials and Methods

See *SI Appendix* for additional materials and methods, figures, and acknowledgments.

Mice. Expression of collagen type I in real time was studied using reporter Col-GFP mice (24). Cell fate mapping of aHSCs was studied using collagen-α2(I)^{Cre} (25) and collagen-α1(I)^{Cre} (*SI Appendix*) and tamoxifen-inducible collagen-α2(I)$^{ER\text{-}Cre}$ crossed to Rosa26$^{flox\text{-}Stop\text{-}flox\text{-}YFP}$ mice (or Rosa26$^{flox\text{-}mTRed\text{-}Stop\text{-}flox\text{-}mGFP}$ mice) (Jackson Labs). GFAP^{Cre} mice were used to determine the total number of HSCs.

Liver Fibrosis. Liver fibrosis was induced in mice by intragastric gavage with CCl_4 (at 16 × 1:4 dilution in 100 μL of corn oil) over 2 mo (8) or by intragastric ethanol feeding combined with Western diet (for 2 mo) (*SI Appendix*) (26). Reversal of liver fibrosis was studied 1 mo after CCl_4 cessation and 7 wk after withdrawal from alcohol feeding. Recurrent injury in Col-GFP mice was induced for 1 mo with CCl_4 (8 × 1:4). Liver injury in $Rag^{-/-}\gamma c^{-/-}$ and $Hspa1a/b^{-/-}$ mice was gradually induced with CCl_4 (4 × 1:16; 2 × 1:8; 2 × 1:4) for 1 mo. Collagen content was measured by hydroxyproline and Sirius Red staining.

Isolation of Nonparenchymal Cell Fraction and Primary HSCs. Livers are perfused and digested using pronase/collagenase and the gradient centrifugation method, as previously described (8). Freshly isolated HSCs were analyzed by flow cytometry or cultured in DMEM (Gibco-BRL) + 10% FCS and 2 mM L-glutamine + antibiotics.

Flow Cytometry. Phenotyping of the hepatic nonparenchymal cells was performed on FACSCanto II RUO (BD). Activated myofibroblasts were visualized by GFP expression (488 nm) using argon laser, and vitamin A^+ expression (405 nm) was detected by violet laser. Cell sorting was performed on a MoFlo (Beckman Coulter) for GFP (488 nm, using Lyt-200S laser, iCYP Visionary Bioscience Inc.) and vitamin A (350 nm, UV laser, JDSU-Excyte).

Whole-Mouse Genome Gene Expression Microarray. The gene expression profile of HSCs was studied using Whole Mouse Genome Microarray (Agilent). Vitamin A^+YFP^+ and vitamin A^+YFP^- HSCs were purified by cell sorting from collagen-α2(I)$^{Cre\text{-}YFP}$ mice with no injury, from mice after CCl_4 treatment (2 mo), and from mice after 7 d or 1 mo recovery from CCl_4. mRNA was purified using RNAeasy columns (Qiagen), and 160 ng of purified RNA per sample was labeled using the LRILAK PLUS and hybridized to a Whole Mouse Genome Microarray 4 × 44,000 60-mer slide (Agilent). Slides were analyzed using the Gene Spring Software (Agilent) as described in *SI Appendix*. Quantitative RT-PCR and apoptosis of aHSCs are described in *SI Appendix*.

1. Bataller R, Brenner DA (2005) Liver fibrosis. *J Clin Invest* 115:209–218.
2. Iredale JP, et al. (1998) Mechanisms of spontaneous resolution of rat liver fibrosis. Hepatic stellate cell apoptosis and reduced hepatic expression of metalloproteinase inhibitors. *J Clin Invest* 102:538–549.
3. Krizhanovsky V, et al. (2008) Senescence of activated stellate cells limits liver fibrosis. *Cell* 134:657–667.
4. Friedman SL, Roll FJ, Boyles J, Bissell DM (1985) Hepatic lipocytes: The principal collagen-producing cells of normal rat liver. *Proc Natl Acad Sci USA* 82:8681–8685.
5. She H, Xiong S, Hazra S, Tsukamoto H (2005) Adipogenic transcriptional regulation of hepatic stellate cells. *J Biol Chem* 280:4959–4967.
6. Lee CG, et al. (2004) Early growth response gene 1-mediated apoptosis is essential for transforming growth factor beta1-induced pulmonary fibrosis. *J Exp Med* 200:377–389.
7. Huby AC, et al. (2009) Restoration of podocyte structure and improvement of chronic renal disease in transgenic mice overexpressing renin. *PLoS ONE* 4:e6721.
8. Seki E, et al. (2007) TLR4 enhances TGF-beta signaling and hepatic fibrosis. *Nat Med* 13:1324–1332.
9. Lee KS, Buck M, Houglum K, Chojkier M (1995) Activation of hepatic stellate cells by TGF alpha and collagen type I is mediated by oxidative stress through c-myb expression. *J Clin Invest* 96:2461–2468.
10. Stefanovic B, Brenner DA (2003) 5′ Stem-loop of collagen alpha 1(I) mRNA inhibits translation in vitro but is required for triple helical collagen synthesis in vivo. *J Biol Chem* 278:927–933.
11. Goldman JP, et al. (1998) Enhanced human cell engraftment in mice deficient in RAG2 and the common cytokine receptor gamma chain. *Br J Haematol* 103:335–342.
12. Hawley TS, Herbert DJ, Eaker SS, Hawley RG (2004) Multiparameter flow cytometry of fluorescent protein reporters. *Methods Mol Biol* 263:219–238.
13. Wright MC, et al. (2001) Gliotoxin stimulates the apoptosis of human and rat hepatic stellate cells and enhances the resolution of liver fibrosis in rats. *Gastroenterology* 121:685–698.
14. Siegmund SV, et al. (2007) The endocannabinoid 2-arachidonoyl glycerol induces death of hepatic stellate cells via mitochondrial reactive oxygen species. *FASEB J* 21:2798–2806.
15. Ikeyama S, Kusumoto K, Miyake H, Rokutan K, Tashiro S (2001) A non-toxic heat shock protein 70 inducer, geranylgeranylacetone, suppresses apoptosis of cultured rat hepatocytes caused by hydrogen peroxide and ethanol. *J Hepatol* 35(1):53–61.
16. Wells RG (2008) The role of matrix stiffness in regulating cell behavior. *Hepatology* 47:1394–1400.
17. Tsukamoto H (2005) Adipogenic phenotype of hepatic stellate cells. *Alcohol Clin Exp Res* 29(11, Suppl)132S–133S.
18. Kalinichenko VV, et al. (2003) Foxf1 +/– mice exhibit defective stellate cell activation and abnormal liver regeneration following CCl4 injury. *Hepatology* 37(1):107–117.
19. Asahina K, et al. (2009) Mesenchymal origin of hepatic stellate cells, submesothelial cells, and perivascular mesenchymal cells during mouse liver development. *Hepatology* 49:998–1011.
20. Yin Z, Wu W, Fung JJ, Lu L, Qian S (2007) Cotransplanted hepatic stellate cells enhance vascularization of islet allografts. *Microsurgery* 27:324–327.
21. Winau F, et al. (2007) Ito cells are liver-resident antigen-presenting cells for activating T cell responses. *Immunity* 26(1):117–129.
22. Yenari MA, et al. (2005) Antiapoptotic and anti-inflammatory mechanisms of heat-shock protein protection. *Ann N Y Acad Sci* 1053:74–83.
23. Gabai VL, et al. (2000) Hsp72-mediated suppression of c-Jun N-terminal kinase is implicated in development of tolerance to caspase-independent cell death. *Mol Cell Biol* 20:6826–6836.
24. Yata Y, et al. (2003) DNase I-hypersensitive sites enhance alpha1(I) collagen gene expression in hepatic stellate cells. *Hepatology* 37(2):267–276.
25. Florin L, et al. (2004) Cre recombinase-mediated gene targeting of mesenchymal cells. *Genesis* 38:139–144.
26. Tsukamoto H, Mkrtchyan H, Dynnyk A (2008) Intragastric ethanol infusion model in rodents. *Methods Mol Biol* 447:33–48.